The Journal of Neuroscience, October 1, 1999, *19*(19):8163–8171

Arachidonic Acid Reciprocally Alters the Availability of Transient and Sustained Dendritic K^+ Channels in Hippocampal CA1 Pyramidal Neurons

Costa M. Colbert and Enhui Pan

Department of Biology and Biochemistry, University of Houston, Houston, Texas 77204-5513

The dendrites of hippocampal CA1 pyramidal cell dendrites express a high density of transient A-type K^+ channels, which play a critical role in the back-propagation of action potentials and in the determination of dendritic excitability. Recently, arachidonic acid and its nonmetabolizable analogue 5,8,11,14-eicosatetraynoic acid (ETYA) were shown to block transient K^+ channels in the somata of these cells (Keros and McBain, 1997), but to have little effect on the somatic action potential. In the present study we have investigated the effects of arachidonic acid and ETYA on the gating of channels and the excitability of the apical dendrites of CA1 pyramidal neurons. We found not only a block of transient K^+ channels, but also an enhancement of sustained outward currents. The sustained currents consisted of at least two distinct channel types. The larger conductance channel (>50 pS) was identified as a K^+ channel. Arachidonic acid greatly enhanced the amplitude of back-propagating dendritic action potentials (>200 μm from the soma) but did not result in sustained depolarizations of the dendrites similar to those seen with 4-aminopyridine (4-AP) application. In fact, arachidonic acid reduced dendritic excitability when applied after 4-AP. Thus, arachidonic acid appears to cause a shift of available channels from the fast, transient type to the slower, sustained types. The net effect appears to be an enhancement of dendritic action potential amplitude that occurs without compromising the electrical stability of the dendrites.

Key words: arachidonic acid; dendrite; single channel recording; potassium channel; pyramidal neuron; electrophysiology; rat

Back-propagating dendritic action potentials provide a rapid means for pyramidal neurons to signal their firing state throughout their extensive dendritic arbors (Jaffe et al., 1992; Stuart et al., 1997; Magee et al., 1998). By providing both a strong postsynaptic depolarization and Ca^{2+} influx, the back-propagating action potential may be critical in signaling the induction of associative processes such as long-term potentiation (Magee and Johnston, 1997; Markram et al., 1997). The amplitude of the dendritic back-propagating action potential, however, is not all-or-none, but decreases steadily as it travels away from the soma (Turner et al., 1991; Spruston et al., 1995; Svoboda et al., 1997; Buzsáki and Kandel, 1998). How far the action potential travels in the dendrites depends strongly on the previous level of dendritic depolarization (Tsubokawa and Ross, 1996; Hoffman et al., 1997; Magee et al., 1998), the postsynaptic firing rate (Callaway and Ross, 1995; Spruston et al., 1995), and the state of various neuromodulatory systems (Tsubokawa and Ross, 1997; Hoffman and Johnston, 1999).

Recent work has identified the ionic mechanisms responsible for the decremental nature of the back-propagating dendritic action potential in CA1 pyramidal neurons. Transient A-type K^+ channels in the apical dendrites, putatively identified as Kv4.2 (Sheng et al., 1992; Maletic-Savatic et al., 1995) (for review, see Hoffman and Johnston, 1998), steadily increase in density with distance from the soma (Hoffman et al., 1997). As the back-propagating action potential travels through the dendrites, it encounters increasing outward current that eventually limits propagation. Thus, modulation of transient K^+ channel properties impacts back-propagation (Hoffman et al., 1997). Activation of either protein kinase A (PKA) or protein kinase C (PKC), for example, alters the voltage dependence of activation of the transient K^+ channels (Hoffman and Johnston, 1998) and thereby alters back-propagation.

In addition to phosphorylation by kinases, Kv4.2 channels (Villarroel and Schwarz, 1996) and transient K^+ channels in CA1 somata (Keros and McBain, 1997) are inhibited by arachidonic acid and its nonmetabolizable analog 5,8,11,14-eicosatetraynoic acid (ETYA). Keros and McBain (1997) demonstrated a dose-dependent block of transient K^+ current associated with an increase in the rate of inactivation in somatic macropatches. However, under normal conditions, they found an absence of effect on the somatic action potential. Given the much higher density of transient K^+ channels in the apical dendrites, we hypothesized that application of arachidonic acid would have a much greater effect on the dendritic action potential. Indeed, we observed a profound increase in action potential amplitude in the presence of arachidonic acid. However, this increase in amplitude was not accompanied by sustained Ca^{2+} spikes that are normally associated with the block of K^+ channels by 4-aminopyridine (4-AP; Hoffman et al., 1997, their Fig. 3). Observing the effects of arachidonic acid on K^+ currents in dendritic cell-attached patches, we found not only inhibition of the rapidly activating transient current, but an enhancement of more slowly activating

Received June 1, 1999; revised July 9, 1999; accepted July 12, 1999.

This work was supported by National Institute of Health Grant NS36982. We thank S. Dryer for comments on an earlier version of this manuscript, J. C. Magee for suggesting the 4-AP experiment, M. Ho for technical assistance, C. J. McBain for helpful discussions regarding the stability of ETYA, and G. W. G. Chase for encouragement early in this study.

Correspondence should be addressed to Dr. Costa M. Colbert, Department of Biology and Biochemistry, University of Houston, 4800 Calhoun Road, Houston, TX 77204-5513.

sustained currents. Thus, arachidonic acid may dynamically regulate the balance of dendritic K^+ currents, allowing a larger back-propagating action potential while maintaining electrical stability of the dendrites.

MATERIALS AND METHODS

Preparation and solutions. The present study used 120–180 gm male Sprague Dawley rats. Animals were anesthetized with a lethal dose of a combination of ketamine and xylazine. Once deeply anesthetized, they were perfused through the heart with cold modified artificial CSF containing (in mM), 110 sucrose, 60 NaCl, 3.0 KCl, 1.25 NaH_2PO_4, 28 $NaHCO_3$, 0.5 $CaCl_2$, 7.0 $MgCl_2$, and 5 dextrose. After removal of the brain, 400-μm-thick slices were cut using a Vibratome (Lancer), incubated submerged in a holding chamber for 30 min at 32°C, and stored submerged at room temperature.

During the slicing procedure, the slices were maintained in the same ACSF as used for the perfusion. The external recording solution contained (in mM) 125 NaCl, 2.5 KCl, 1.25 NaH_2PO_4, 25 $NaHCO_3$, 2.0 $CaCl_2$, 1.0 $MgCl_2$, and 25 dextrose. Slices were maintained in a submerged holding chamber in the normal external recording solution. All external solutions were bubbled continuously with 95% O_2 and 5% CO_2. The internal pipette solution used for whole-cell recordings contained (in mM), 140 KGluconate, 10 HEPES, 1 EGTA, 4.0 NaCl, 4.0 Mg_2ATP, 0.3 Mg_2GTP, and 14 phosphocreatine. pH was adjusted to 7.25 with KOH. For recording K^+ currents in the cell-attached configuration, the pipette contained (in mM), 130 NaCl, 10 HEPES, 2 $CaCl_2$, 1 $MgCl_2$, 2.5 KCl, and 1 μM tetrodotoxin (TTX). pH was adjusted to 7.4 with NaOH. Where indicated, 10 mM tetraethylammonium (TEA) and/or 1 mM 4-AP was included, or TTX was excluded from the pipette solution. For recording K^+ currents in the inside-out configuration, the pipette solution contained (in mM), 76 NaCl, 10 HEPES, 2 $CaCl_2$, 1 $MgCl_2$, 37.5 KCl, and 1 μM TTX. The bath solution for inside-out recordings eliminated CaCl, added 10 mM EGTA, and replaced NaCl with 134 mM KCl. Synaptic receptor antagonists (see below) and TTX were also included to limit activity in the slice. Inside-out patches were made in normal extracellular solution. After the seal was made, the bath solution was switched to the high-K^+, low Ca^{2+} solution, and the patch was ripped off the cell.

Arachidonic acid (AA; sodium salt) and ETYA (free acid) were obtained from Sigma (St. Louis, MO). AA was dissolved in water or ethanol. ETYA was dissolved in dimethylsulfoxide (DMSO). Stock solutions of ~10 mM were made and divided into aliquots, which were kept in a −80°C freezer. Both substances were extremely labile. Once this fact became apparent, stock solutions were thawed, brought to final concentrations, vortexed, and added to the reservoir during acquisition of control data. When added to the cell-attached pipettes, freshly thawed drug was added to the pipette solution just before filling the pipette. This protocol improved the consistency of the effects dramatically. Final concentration of DMSO was <0.5%. DMSO was washed into the bath without effects on currents in the cell-attached patch ($n = 2$). Bovine serum albumin (BSA; 1 mg/ml; Sigma), which binds fatty acids, was added to the bath to aid recovery.

Recording techniques. Recordings were made from somata and dendrites of hippocampal CA1 pyramidal neurons. Neurons were visualized using infrared illuminated, differential interference contrast (DIC) optics (Olympus Optical, Tokyo, Japan) according to standard techniques (Stuart et al., 1993). Whole-cell patch recordings were made using microelectrode amplifiers (BVC-700; Dagan Instruments) in bridge mode. Cell-attached patch recordings were made using a patch-clamp amplifier with a capacitive headstage (Axopatch 200; Axon Instruments, Foster City, CA). Pipettes (3–5 MΩ for whole-cell; 7–12 MΩ for cell-attached) were made from borosilicate glass (Warner Glass) and pulled using a P-87 Flaming-Brown pipette puller (Sutter Instruments) and coated with Sylgard (Dow Corning). Most cell-attached patch recordings were made at room temperature (~25°C). Whole-cell recordings were made at 30–32°C. Whole-cell series resistance was 6–20 MΩ for somatic recordings and 15–40 MΩ for dendritic recordings. All cells used had initial resting membrane potentials negative to −60 mV, and typically were in the range of −65 to −70 mV. Whole-cell recordings were low-pass filtered at 3 kHz (6 dB/octave) and digitized at 10 kHz. Cell-attached patch recordings were filtered at 2 kHz (8 pole Bessel filter) and sampled at 10 kHz. Data were digitized at 16 bit resolution (ITC-18; Instrutech) and stored by computer for offline analysis (Next Computer). Nonlinear curve fits and statistical tests were made using Mathematica (Wolfram). Significance was determined by t test with $p < 0.05$ considered significant. Data are reported as mean ± SEM.

K^+ currents were recorded in the cell-attached and inside-out configurations. Typically, patches were held at −30 mV negative to the resting potential of the cell to remove inactivation of transient channels. Potentials reported are the transmembrane potentials. Effects of the drugs were observed using command potentials of +20–50 mV. Ensemble averages were calculated from 30–50 sweeps unless otherwise noted. Leak currents were determined by scaling smaller (20 mV) steps digitally offline. Leak steps were interleaved with test steps continuously throughout each experiment to monitor any changes in leak currents. Membrane potentials were determined when possible by rupturing the patch after data collection and were in the range of −65 to −70 mV. As an additional test of depolarization of the cell during cell-attached recordings, the patch was held hyperpolarized at −50 mV and stepped to the same command potentials. If an increase in transient current was noted, the cell was assumed to have depolarized, and the patch was excluded from further analysis. Patches were also excluded if capacitive currents caused by cell firing were detected. Reported transient K^+ current amplitudes were measured at the peak of the current waveform current. Sustained current amplitudes were measured as the mean value of current in the last 10 msec of the depolaring voltage command, ~150 msec.

Antidromic action potentials were stimulated by constant current pulses (Neurolog; Digitimer Ltd.; 70–500 μA) through monopolar tungsten electrodes (AM Systems) placed in the alveus. Positioning of the stimulating electrodes and the intensity of stimulation minimized synaptic activation. To limit any synaptic activation during antidromic stimulation, the glutamate receptor antagonists 6,7-dinitroquinoxaline-2,3-dione (DNQX; 10 μM) and 2-amino-5-phosphono-valeric acid (AP-5; 50 μM) and the $GABA_A$ receptor antagonist bicuculline methiodide (10 μM) were routinely added to the extracellular solution. Antagonists were obtained from Sigma.

RESULTS

ETYA increases the amplitude of the back-propagating dendritic action potential

Rapidly inactivating K^+ channels play a critical role in shaping back-propagating dendritic action potentials in CA1 pyramidal neurons (Hoffman et al., 1997). Therefore, we hypothesized that blockade of the transient K^+ channels by arachidonic acid should increase the amplitude of back-propagating action potentials. Interpretation of arachidonic acid actions is complicated by the fact that it is rapidly metabolized to form intermediates that are important second-messengers in a variety of processes. Thus, to aid the interpretation of the results by reducing the range of metabolites produced, we used an analogue of arachidonic acid, ETYA, that is not a substrate for the major metabolic pathways of arachidonic acid. ETYA has been demonstrated previously to block transient K^+ channels with an efficacy and potency similar to arachidonic acid (Villarroel and Schwarz, 1996; Keros and McBain, 1997; Dryer et al., 1998).

To observe the effects of ETYA on the back-propagating action potential, we made whole-cell recordings from the apical dendrites of CA1 pyramidal cells 200–225 μm from the soma. Antidromic action potentials were evoked (0.1 Hz) by a stimulating electrode placed in the alveus. After recording 20–30 dendritic action potentials, the bath solution was switched to a solution containing ETYA (40 μM). The amplitude of the back-propagating action potential increased to 142 ± 9% of its control value ($n = 5$). Figure 1 shows an example of the effect of ETYA and its reversibility with washout. Figure 2*A* shows additional examples of back-propagating dendritic action potentials before and after application of ETYA. In two cases, the back-propagating action potentials reached ~100 mV, comparable to a somatic action potential. Application of ETYA, however, did not simultaneously increase the maximum rate of rise of the dendritic action potential (4 ± 3%; $n = 5$; Fig. 1*B*). This finding suggests

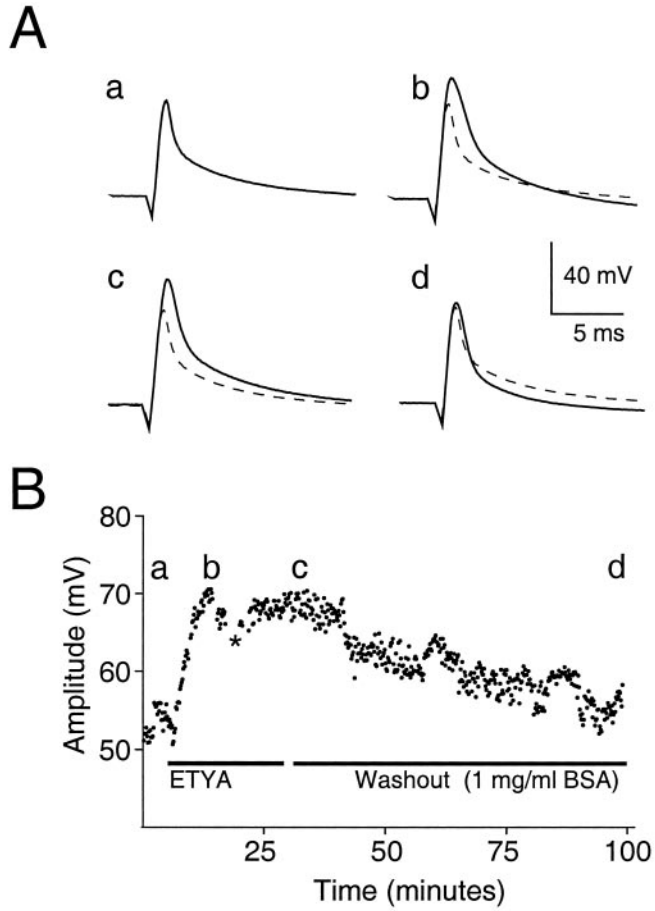

Figure 1. Bath application of ETYA reversibly increases the amplitude of the back-propagating action potential. Whole-cell recording from the apical dendrite 200 μm from the soma. Action potentials were evoked by a stimulating electrode in the alveus. *A*, *a*, Control dendritic action potential. In the remaining panels, this waveform is shown as a *dotted line* for comparison. *b*, ETYA (40 μM) increases the amplitude of the dendritic action potential. *c*, Dendritic action potential before washout begins. *d*, After washout the dendritic action potential has similar amplitude to the control action potential. Bovine serum albumin (1 mg/ml) was added to the bath to aid washout. *B*, Time course of bath application of ETYA experiment. Graph plots the amplitude of the dendritic action potential during the experiment. *Letters* above the plot identify the points corresponding to the waveforms in *A*. After the action potential increased, the electrode series resistance began to increase. The electrode was cleared (*asterisk*), and a new baseline was achieved before washout began. Membrane potential was held at −65 mV throughout the experiment.

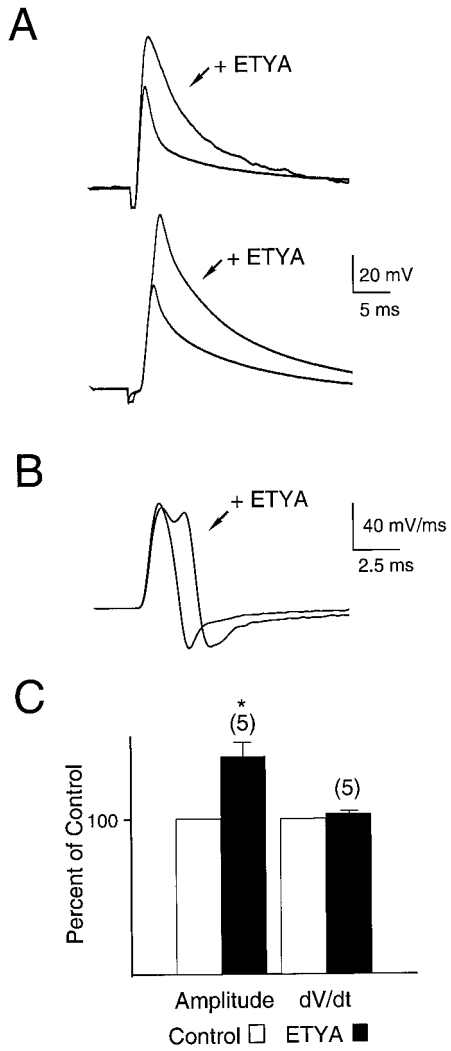

Figure 2. Bath application of ETYA increases dendritic action potentials but not maximum rate of rise. *A*, Results from two cells showing that ETYA (40 μM) can increase the amplitude of the back-propagating dendritic action potential to nearly that of a somatic action potential (90–100 mV). Note, however, that there was no Ca^{2+} spike triggered by these large dendritic spikes, as seen when dendritic action potential amplitude is increased by 4-AP (compare Fig. 10) *B*, Despite the increase in amplitude, the maximum rate of rise of the action potential (dV/dt) does not increase. Rates of rise were computed by subtraction of successive data samples. *C*, Summary of bath application of ETYA (n = 5 cells). Significant changes are marked with an *asterisk*.

that the increase in dendritic action potential amplitude is caused by a decrease in K^+ conductance rather than an increase in Na^+ conductance (cf. Colbert et al., 1997). Figure 2*C* summarizes the results of bath application of ETYA.

Bath application of arachidonic acid (30 μM) or phospholipase (PLA_2; 2 U/ml), which releases arachidonic acid from cell membranes, also increased the amplitude of the back-propagating dendritic spike. Arachidonic acid increased the magnitude of the spike to 137 ± 18% (n = 3) of control. PLA_2 increased the magnitude of the spike to 153 ± 27% (n = 2) of its control value.

Arachidonic acid and ETYA alter dendritic outward currents

Keros and McBain (1997) characterized the effects of arachidonic acid and ETYA on transient channels in macropatches from CA1 somata. Our intent here was not to repeat this entire characterization in the dendrites, but to verify that arachidonic acid and ETYA blocked transient K^+ channels in the apical dendrites (i.e., >200 μm from the soma). We chose to use cell-attached patches in order to preserve the normal cytoplasmic environment of the channels, avoiding such complicating factors as cysteine oxidation (noted by Keros and McBain, 1997). The major disadvantage of cell-attached patches is that bath-applied drug must penetrate the cell within the slice and reach channels that are pulled up into the recording pipette during the lifetime of the patch.

Initially, we tested the block of transient K^+ channels by comparing K^+ currents across two groups of cell-attached patches. The test group included ETYA (40 μM) in the pipette solution. K^+ currents were evoked by voltage steps from a holding potential of −90 mV to a command potential of +30 mV. To normalize for differences in the size of the patches, we calculated

the ratio of the peak transient current amplitude to the sustained current amplitude for each patch. If ETYA blocks the transient current, then this ratio should be decreased. The ratio of the peak transient current to sustained current in the control group was 4.7 ± 1.0 (n = 8). Two small control patches were excluded because the sustained current amplitude was essentially zero, yielding very high ratios. In contrast, the ratio of the peak transient current to the sustained current for the ETYA group was (1.7 ± 0.5; n = 7). Thus, the ratio for the ETYA group was significantly smaller than that of the control group, supporting the hypothesis that the transient current was reduced by ETYA. However, the group averages suggested that ETYA might have had an additional effect. Although not quite reaching our definition of significance, the sustained current (7.1 ± 1.6 pA; n = 8) was greater than the sustained current in the control group (3.6 ± 1.0 pA; n = 10; $p < 0.06$). Thus, we reasoned that the ratio of amplitudes might be decreased not only by the blockade of transient current, but also by an enhancement of the sustained current.

To investigate the actions of ETYA further, we bath-applied ETYA to provide within-patch controls. After data were collected in the normal extracellular solution, we switched to extracellular solution containing ETYA (30 μM). In the first set of patches we observed the effects of ETYA on pharmacologically isolated transient current. In addition to TTX, 4-AP (1 mM) was included in the pipette solution to block slower transient currents (i.e., D-current) and TEA (10 mM) was included to block delayed rectifier-type currents. ETYA significantly reduced the amplitude of the isolated transient current to 46.2 ± 18.4% (n = 5) of control. The time constant of inactivation, as fit by a single exponential, also decreased significantly to 61 ± 11% (n = 5) of control from an initial value of 13.4 ± 3.0 msec. Figure 3 is an example of such an experiment.

In a second set of patches we looked for other effects of ETYA by excluding K^+ channel blockers from the patch pipette (Fig. 4). After bath-applying ETYA, there was an initial increase in the sustained outward current. After a few minutes, the transient current decreased while the sustained current remained increased. The increase in sustained current was seen in three of the five patches observed. In the remaining two patches there was essentially no change in the sustained current. Figure 4*B* summarizes the experiment. The transient current decreased significantly to 70.4 ± 10.7% (n = 5) of control, whereas the sustained current increased significantly to 153.3 ± 23.5% (n = 5) of control.

To verify that arachidonic acid has the same effect as ETYA on dendritic K^+ channels, we repeated the bath application experiment using 30 μM arachidonic acid (Fig. 5*A*). Arachidonic acid significantly decreased the amplitude of the transient current to 52.1 ± 15.7% (n = 7) of its control value. The inactivation time constant fit by a single exponential significantly decreased to 56.9 ± 15.5% of its control value of 13.6 ± 2.1 (n = 4) msec. As in the ETYA experiment, the sustained current increased in four of seven of the patches. The increase in the sustained current was 163.7 ± 41% (n = 6) of its control value. The arachidonic acid experiment is summarized in Figure 5*B*. Pooling the data from the two sets of experiments, bath application of fatty acids increased the sustained current to 158.9 ± 23.7% of the control value (n = 12; $p < 0.016$; one-tailed test).

Keros and McBain (1997) suggested that the block of the somatic transient K^+ channels by arachidonic acid was not caused by a shift in the activation curve. This differs from modulation of

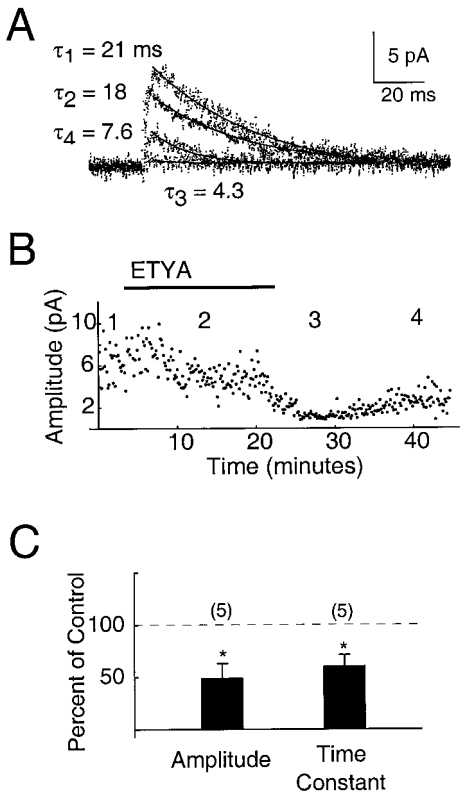

Figure 3. Bath application of ETYA (40 μM) decreases the amplitude of fast, transient A-type K^+ channel currents in cell-attached dendritic patches. Cell-attached patch from apical dendrite ~200 μm from the soma. Sustained and slowly inactivating K^+ currents were blocked with 4-AP (1 mM) and TEA (10 mM) in the patch pipette solution. Transient K^+ currents were evoked by voltage steps from −90 to +30 mV. *A*, Kinetics during progressive block by ETYA. Ensemble averages of 10 sweeps are shown superimposed. *Solid lines* are exponential fits of the data. Time constants given are single exponential time constants. Data were well-fit by single exponentials. The time constant decreases with block of the channels. *B*, Time course of bath application experiment. The graph plots the peak amplitude of the transient current throughout the experiment. ETYA was switched off as soon as an effect was detected to aid washout. *Numbers* above the plot correspond to the ensemble averages and time constants shown in *A*. *C*, Summary of ETYA effect on transient current (n = 5 cells).

the dendritic transient K^+ channels by kinases (Hoffman and Johnston, 1998), which appear to act by shifting the activation curve. Thus, we obtained activation curves for the transient K^+ current before and during the arachidonic acid experiment just described. Assuming a K^+ reversal potential of approximately −95 mV, the conductance at +40 mV was 93 ± 0.5% (n = 6) of the value at +50 mV, the greatest depolarization we used to construct the activation plots. Although there was an ~50% block of the transient current (as described above), there was no shift in the normalized activation curves (Fig. 5*C*). Least-squares fits of Boltzmann functions yielded half-maximal activations at 3.9 and 1.7 mV and slopes of k = 15.6 and k = 15.4 before and after application of arachidonic acid, respectively.

Examining individual current traces before and after the bath application of arachidonic acid and ETYA yielded additional information about the nature of the sustained currents. In most patches, individual openings were not well resolved. However, in some patches only a few channels contributed to the sustained ensemble current. These patches revealed more than one source

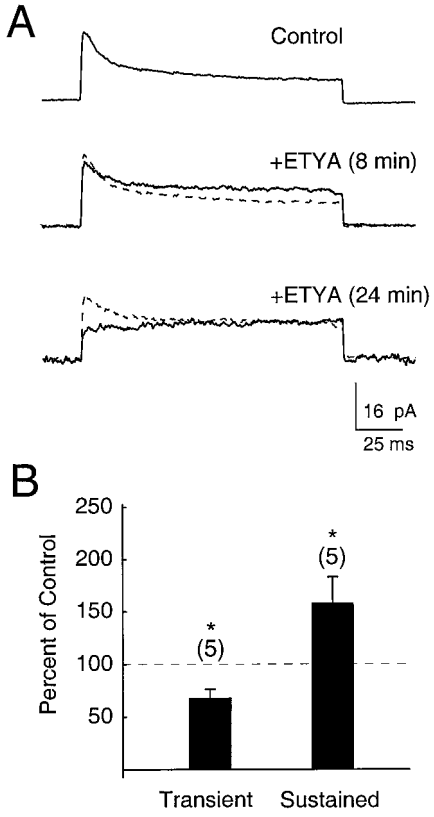

Figure 4. Bath application of ETYA (40 μM) enhances sustained current while decreasing transient current. *A*, *Top panel*, K^+ currents were evoked by voltage steps from −90 to +30 mV. No K^+ channel blockers were included in the patch pipette. *Top panel*, Waveform is ensemble average of 30 sweeps in control solution, showing transient and sustained currents. *Middle panel*, Solid waveform is ensemble average of 15 sweeps beginning 8 min after start of bath application of ETYA, showing an increase in the sustained current and a small decrease in the transient current. *Bottom panel*, Solid waveform is ensemble average of 15 sweeps beginning 24 min after the start of ETYA. The 8 min waveform is shown as a *dotted line* for comparison. There is no further increase of the sustained current, but the transient current continues to decrease in amplitude. *B*, Summary of the ETYA effect on transient and sustained outward currents after 20–30 min exposure.

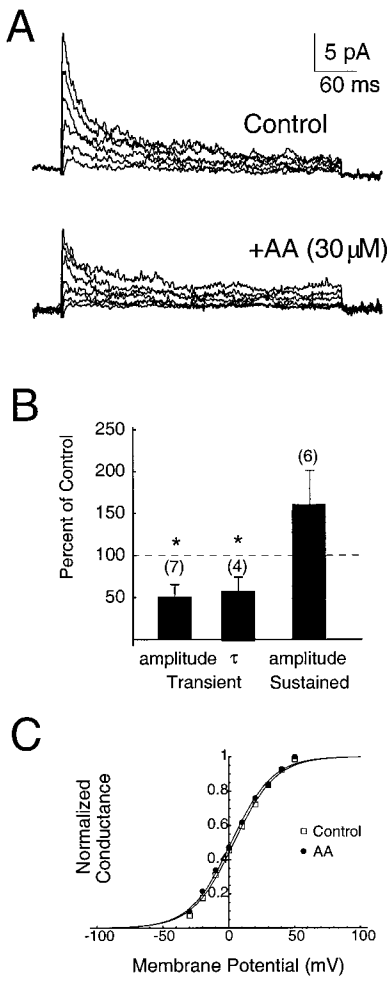

Figure 5. Bath application of arachidonic acid (30 μM) enhances sustained current while decreasing transient current. *A*, *Top panel*, Ensemble averages of 12 sweeps in control conditions for steps from −90 mV to command potentials from −30 to +50 mV. *Bottom panel*, Ensemble averages of 15 sweeps after application of arachidonic acid. *B*, Summary of experiment. Arachidonic acid decreased the amplitude of the transient current and the inactivation time constant (τ), while increasing the amplitude of the sustained current. *C*, Activation curves for the transient currents before (*open squares*) and after (*filled dots*) application of arachidonic acid. Block of the transient current was not associated with a significant shift in the activation curve. Error bars were approximately the size of the symbols. Lines represent least-squares fit to Boltzmann (see Materials and Methods).

of additional current. Figure 6 shows the first. The top panel of Figure 6*A* shows ensemble averages before and after application of ETYA. The bottom panels show examples of single sweeps in which single channel openings can be seen. Figure 6*B* shows the individual data samples superimposed. The data points begin 80 msec after the voltage command to allow the transient current to decay (i.e., Fig. 6*A* between the *arrows*). Favored levels can be seen as a high density of samples. Application of ETYA resulted in a shift of the favored levels to higher current. An all-points histogram made from these data (Fig. 6*C*) suggests that the favored current levels are multiples of 1.9 pA or ~15 pS. Application of ETYA resulted in a shift in the favored levels to another multiple of 1.9 pA, consistent with either an increased probability of opening of channels in the patch or the recruitment of an additional channel of similar unitary conductance. A similar shift in discrete current levels was noted in two additional patches.

The second source of outward current that appeared after the application of ETYA or arachidonic acid was associated with large-conductance channel openings. Figure 7 shows an example of such a channel. Figure 7*A* shows 15 consecutive superimposed sweeps in the control condition and their resulting ensemble average. Figure 7*B* shows 15 consecutive sweeps from the same patch after the application of arachidonic acid and the resulting ensemble average. A new favored current level appears, increasing the sustained current in the ensemble average. Figure 7*C* shows individual traces, suggesting that these increases in current are caused by openings of a large-conductance channel. From the linear portion of the IV plot, the unitary conductance of this channel was 55 pS.

Finally, to determine whether the fatty acid-activated currents were carried by K^+ ions, we applied ETYA to inside-out patches. We used a pipette solution of relatively high K^+ to limit rectification of the channels, and thus, allow us to determine the reversal potential. Figure 8 shows an example of such a recording. The patch was held at −30 mV and stepped to a command

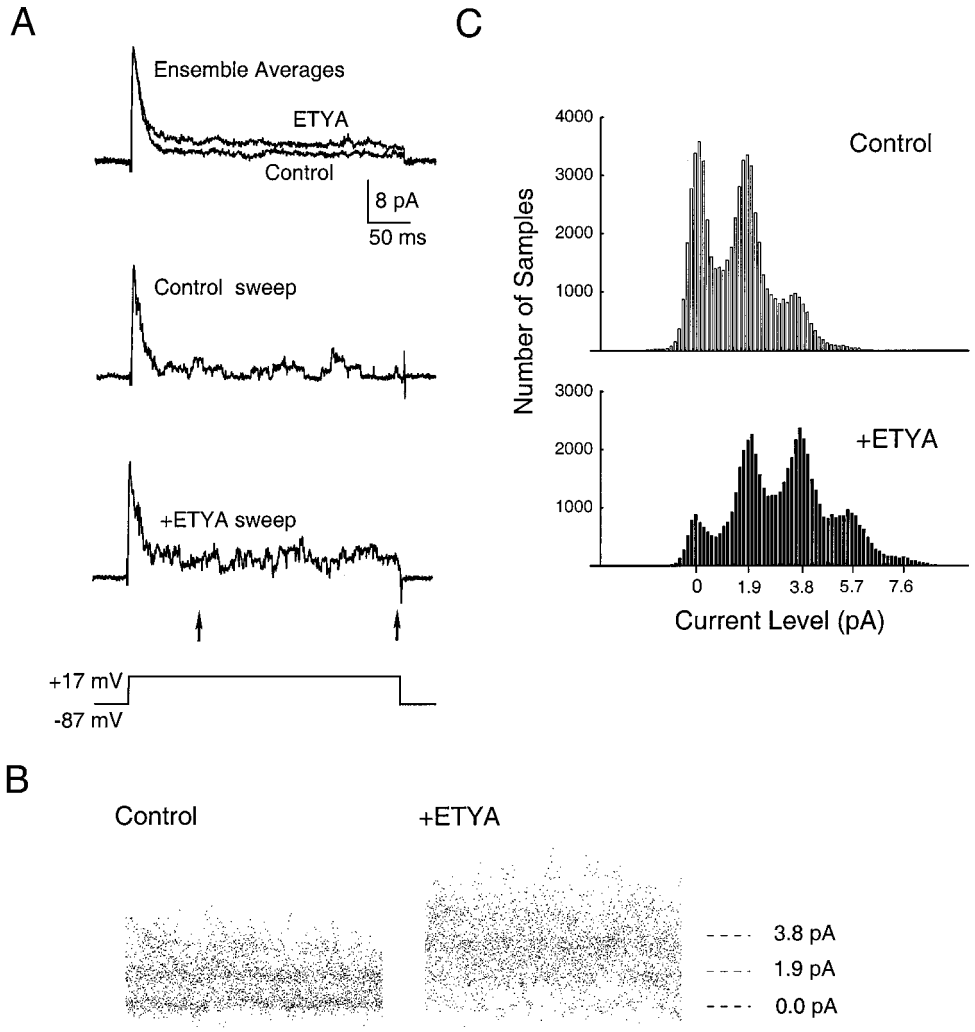

Figure 6. Enhancement of sustained current by a small conductance channel. *A*, *Top panel*, K^+ currents in a cell-attached patch ~200 μm from the soma evoked by a step from −87 to +17 mV. Ensemble averages of 25 sweeps before and after application of ETYA showing enhancement of sustained current. *Middle* and *Bottom panels*, Individual sweeps show clear openings and closings of sustained channels. *B*, Plotting the sample points beginning 80 msec after the step depolarization (*A*, between the arrows) demonstrates two favored levels of current for the sustained channels, and a shift in the favored level after ETYA application. *C*, Plotting these data as all-points histograms indicates clear peaks at multiples of 1.9 pA (~15 pS). After ETYA there is a shift in the favored level, but the same peaks are maintained. Thus, the additional conductance may be caused by increased opening of the same channels or activation of additional channels of similar conductance.

potential of +40 mV once each 3 sec. After application of ETYA, a large-conductance outward current appeared. From the IV plot, (Figure 8*B*,*C*) the conductance was determined to be 89 pS, and the reversal potential was −39 mV. This reversal potential corresponds closely to the calculated K^+ equilibrium potential of −35 mV. In some patches, ETYA activated a smaller conductance channel with a unitary conductance of 16 pS. This channel is probably identical to the smaller conductance channel seen in the cell-attached recordings. In each case, the currents reversed at approximately −40 mV, suggesting that they are carried by K^+ channels.

Redistribution of outward current increases action potential amplitude while maintaining membrane stability

In previous studies, the amplitude of the dendritic back-propagating action potential was increased by blocking transient K^+ current with 4-AP (Colbert et al., 1997; Hoffman et al., 1997). These large action potentials were invariably accompanied by sustained Ca^{2+}-dependent plateau potentials in the dendrites and eventually by an inability of the cell to repolarize. In contrast, application of ETYA and arachidonic acid greatly increased the amplitude of the back-propagating spike (Figs. 1, 2), but did not induce sustained depolarizations and bursts. We hypothesized that the enhancement of the sustained current by arachidonic acid and ETYA might limit these bursts. To test this idea, we observed the effect of arachidonic acid on bursting and on sustained depolarizations induced by previous application of 4-AP (Fig. 9; n = 5). Whole-cell dendritic recordings were made at >200 μm from the soma to monitor back-propagating action potentials. 4-AP (4 mM) added to the bath increased the amplitude of the back-propagating action potential. Once the effect of 4-AP began, sustained depolarizations of the dendritic membrane followed nearly every back-propagating action potential. In all but one cell, subsequent application of arachidonic acid (30 μM) shortened the bursts and decreased the probability of evoking bursts. In the example shown (Fig. 9*C*), bursts were eventually blocked completely. The amplitude of the back-propagating action potential remained greatly increased as expected from the block of transient K^+ current by both 4-AP and arachidonic acid.

To further investigate the relationship of transient and sustained currents to dendritic membrane stability, we observed the effects of ETYA and arachidonic acid during a partial block of the sustained currents with TEA (4–10 mM). TEA was either included in the whole-cell patch pipette (n = 4) or bath-applied (n = 3). TEA alone did not cause bursting or sustained depolarizations when applied alone (data not shown). Figure 10 shows an example of serial bath application of arachidonic acid and TEA. Bath application of arachidonic acid (30 μM) decreased the threshold for action potential initiation in response to a dendritic current injection (Fig. 10*A*, *top* and *middle* panels), but did not

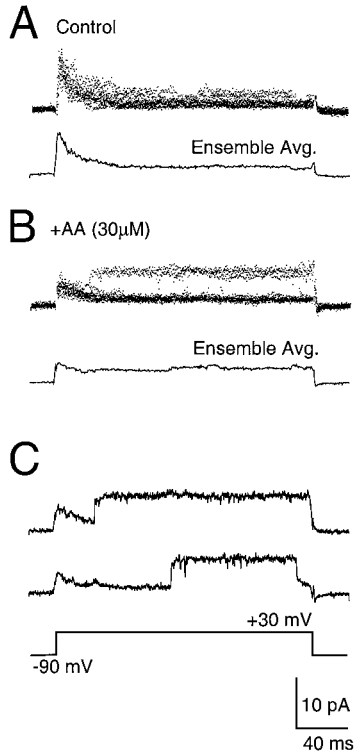

Figure 7. Enhancement of sustained current by a large conductance channel. *A*, K^+ currents in a cell-attached patch ~200 μm from the soma evoked by a step from −90 to +30 mV. *A*, *Control*, 10 superimposed consecutive sweeps and their ensemble average showing transient and sustained currents. *B*, 10 superimposed consecutive sweeps and their ensemble average after bath application of arachidonic acid. Note that transient currents decrease and a new favored level appears, enhancing the sustained current in the ensemble average. *C*, Individual sweeps from *B* show the favored level results from the opening of a larger conductance channel (~55 pS).

result in sustained depolarizations. Subsequently adding TEA (4 mM) to the bath quickly resulted in a sustained depolarizing plateau potential. These results suggest that the sustained current is important in maintaining membrane stability when the transient current is decreased either by modulation or by activity-dependent inactivation. Furthermore, it suggests that the decrease in bursting seen in the 4-AP and arachidonic acid experiment above is not likely caused by blockade of Ca^{2+} channels by arachidonic acid.

DISCUSSION

Decremental back-propagating action potentials have been extensively studied in the apical dendrites of pyramidal neurons in both hippocampus and neocortex (Turner et al., 1991; Stuart and Sakmann, 1994; Spruston et al., 1995; Buzsáki et al., 1996; Svoboda et al., 1997). Although the full range of their function is not fully understood, a potential role as a rapid, long-range intracellular signal for synaptic plasticity has been demonstrated (Magee and Johnston, 1997). Perhaps the most intriguing aspect of the back-propagating action potential as an intracellular signal is that it is highly conditional. That is, both the history of activity (Callaway and Ross, 1995; Spruston et al., 1995; Colbert et al., 1997; Hoffman et al., 1997; Magee and Johnston, 1997) and the state of various neuromodulatory systems (Tsubokawa and Ross, 1997; Hoffman and Johnston, 1999) greatly determine the efficiency of back-propagation. Thus, the back-propagating action

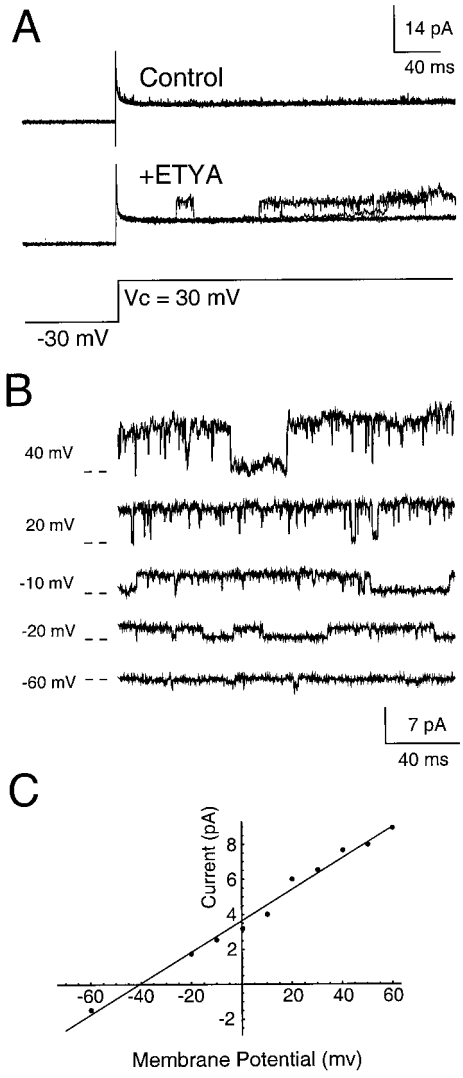

Figure 8. Reversal potential of large-conductance channel activated by ETYA. Currents in an inside-out patch from ~150 μm from soma. Pipette solution included high K^+ to decrease rectification and allow an estimate of the reversal potential. *A*, The patch was held at −30 mV to inactivate transient currents and stepped to a command potential of +30 mV. Waveforms are 15 consecutive individual sweeps before (*control*) and after (*ETYA*) application of ETYA (40 μM) to the bath. Data are not leak-subtracted. *B*, Representative traces at various potentials to show single-channel openings. Patch was held at −90 mV and stepped to potentials from −60 to +60 mV as indicated. Waveforms begin ~50 msec after the step. *C*, I–V plot constructed from unitary currents as in *B*. From the best fit line, the slope yields a conductance of 89 pS, and the current reverses near −40, near the calculated equilibrium potential for K^+.

potential provides a critical regulatory substrate for the control of synaptic plasticity.

Recent work has identified the transient A-type K^+ channels, primarily of the Kv4.2 subtype (Sheng et al., 1992; Maletic-Savatic et al., 1995; Serôdio et al., 1996), as the major determinant of dendritic action potential amplitude in CA1 pyramidal neurons (Hoffman et al., 1997). First, blockade of the transient current with 4-AP dramatically increased the amplitude of dendritic action potentials, although the high concentrations required are not completely selective for transient K^+ channels. Second, right-shifting the activation curve of the transient current by protein kinases is associated with an increase in action potential ampli-

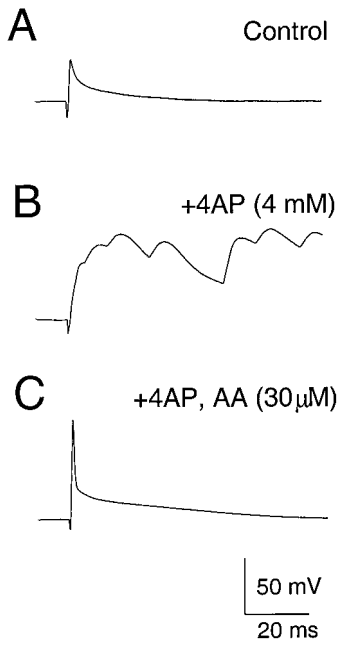

Figure 9. Arachidonic acid decreases the sustained depolarizations and bursts resulting from K^+ channel blockade by 4-AP. Whole-cell recording from apical dendrite ~200 μm from the soma. Back-propagating action potentials were evoked by a stimulating electrode in the alveus. *A*, Antidromic stimulation evokes a back-propagating action potential in the dendrites. *B*, Bath application of 4-AP (4 mM) increases the amplitude of the dendritic action potential, but results in large, sustained Ca^+ spikes. *C*, Approximately 15 min after application of arachidonic acid (30 μM), the sustained depolarizations were completely blocked, leaving a single back-propagating action potential nearly twice the amplitude it had in the initial control condition.

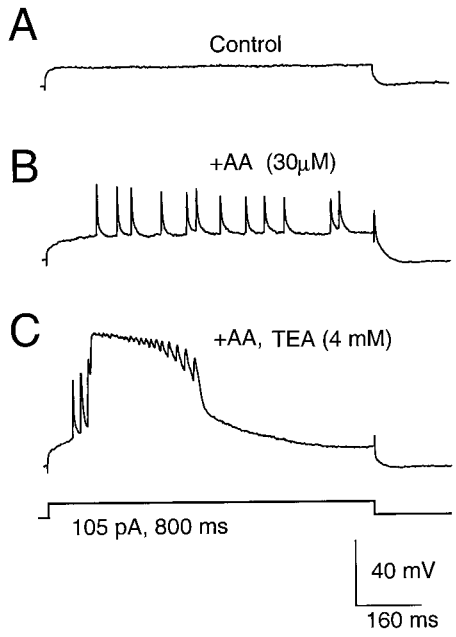

Figure 10. Block of sustained currents produces sustained depolarizations. Whole-cell recording from an apical dendrite ~200 μm from the soma. Current was injected through the dendritic recording electrode to depolarize the dendrite. *A*, In the control condition the current injection was below the threshold for initiating action potentials. *B*, Bath application of arachidonic acid lowered the threshold for initiating action potentials. Note that there was some tendency for spikes to cluster, but no sustained bursts. *C*, Subsequent addition of TEA (4 mM) to the bath to block sustained currents allowed sustained depolarizations to occur. Thus, sustained currents contribute to membrane stability when transient currents are reduced. These data also demonstrate that Ca^{2+} currents, which may be reduced by arachidonic acid, are still sufficient under these conditions to produce a sustained depolarization.

tude (Hoffman and Johnston, 1998). Third, computer simulations suggest that the relatively slow activation kinetics of the sustained currents have little effect on dendritic action potential amplitude (Hoffman et al., 1997). Finally, the present results support a role for transient channels in shaping the dendritic action potential. Block of transient K^+ channels increased dendritic action potential amplitude although the sustained K^+ currents increased.

In addition to providing postsynaptic depolarization sufficient to open NMDA-receptor channels, back-propagating action potentials, if sufficiently large, lead to an influx of Ca^+ in the dendrites (Spruston et al., 1995; Tsubokawa and Ross, 1997; Magee et al., 1998). Although the exact importance is unclear, block of L-type Ca^+ channels reduces synaptic plasticity in at least one paradigm (Magee and Johnston, 1997). Under conditions in which dendritic K^+ channels are reduced in number, for example by 4-AP, this activation of Ca^{2+} channels can lead to sustained depolarizations, firing, and even death of the cell. Thus, if the neuron is to allow a relatively large spike to propagate, it must still maintain electrical stability in the dendrites. A shift in the activation range of transient channels (Hoffman and Johnston, 1998) results in a larger action potential, but the increase in spike amplitude opens more K^+ channels, resulting in controlled excitability. In the case of arachidonic acid (or 4-AP), however, there is a block of the channels rather than a shift in the activation curve. Under these conditions, stability can be lost (as in Fig. 10) because additional depolarization activates fewer channels at all potentials. One solution for the cell to maintain stability would be to provide an additional current—one with kinetics too slow to reduce the amplitude of the dendritic action potential. In the present study, we have observed such an effect in the presence of arachidonic acid. The rapidly-activating, transient, A-type currents are reduced while the slower, sustained currents are enhanced. Consequently, the dendritic action potential is larger and can bring in more Ca^{2+}, but the likelihood of prolonged or uncontrolled spikes is diminished.

Effects of arachidonic acid have been reported on a number of different channel types in a number of different cells (Meves, 1994). In addition to the block of transient K^+ channels (Villarroel and Schwarz, 1996; Keros and McBain, 1997; Dryer et al., 1998), arachidonic acid has been shown to activate large conductance channels (>100 pS) directly in cardiac muscle (Kim and Clapham, 1989) and in visual cortical neurons (Horimoto et al., 1997), a small conductance channel (23 pS) in smooth muscle (Ordway et al., 1989), $BK_{(Ca)}$ channels in rat pituitary cells (Duerson et al., 1996), and M-current through lipoxygenase or cyclooxygenase metabolites in hippocampal neurons (Schweitzer et al., 1990). Thus, the present results extend the list of effects of arachidonic acid on K^+ channels and provide some insight into the physiological function of altering the relative availability of different K^+ channel classes.

Although its role in synaptic plasticity remains undefined, arachidonic acid clearly plays a role in altering excitability under conditions that induce long-term potentiation. Arachidonic acid has been shown to modulate synaptic transmission by potentiating NMDA receptor currents (Miller et al., 1992), increasing glutamate release (McGahon and Lynch, 1996), and inhibiting

reuptake of amino acids (Breukel et al., 1997). In fact, it has been argued that a replaceable loss of arachidonic acid in the cell membrane during aging makes the induction of experimental synaptic plasticity more difficult (McGahon et al., 1997). Also relevant to signaling, arachidonic acid appears to modulate both high- and low-threshold Ca^{2+} channels (Keyser and Alger, 1990; Meves, 1994). Thus, the redistribution of available K^+ channel conductances seen here is part of a larger constellation of effects of arachidonic acid to alter the excitability and function of the cell under specific conditions.

Comparing the present results with those of Keros and McBain (1997) highlights the spatial differences in activity and function in the subcellular compartments of the neuron. Although Keros and McBain demonstrated a strong effect of arachidonic acid on the isolated somatic transient K^+ current, they observed little or no effect on somatic action potentials recorded in normal conditions. Rather than being contradictory, the differences in the effects on the somatic and dendritic action potentials are consistent with slower kinetics of the dendritic action potential and the fivefold difference in transient K^+ channel density found across the somatodendritic axis (Hoffman et al., 1997).

REFERENCES

Breukel AI, Besselsen E, Lopes da Silva FH, Lopes da Silva FH, Ghijsen WE (1997) Arachidonic acid inhibits uptake of amino acids and potentiates PKC effects on glutamate, but not GABA, exocytosis in isolated hippocampal nerve terminals. Brain Res 773:90–97.

Buzsáki G, Kandel A (1998) Somadendritic backpropagation of action potentials in cortical pyramidal cells of the awake rat. J Neurophysiol 79:1587–1591.

Buzsáki G, Penttonen M, Nádasdy Z, Bragin A (1996) Pattern and inhibition-dependent invasion of pyramidal cell dendrites by fast spikes in the hippocampus in vivo. Proc Natl Acad Sci USA 93:9921–9925.

Callaway JC, Ross WN (1995) Frequency-dependent propagation of sodium action potentials in dendrites of hippocampal CA1 pyramidal neurons. J Neurophysiol 74:1395–1403.

Colbert CM, Magee JC, Hoffman DA, Johnston D (1997) Slow recovery from inactivation of Na^+ channels underlies the activity-dependent attenuation of dendritic action potentials in hippocampal CA1 pyramidal neurons. J Neurosci 17:6512–6521.

Dryer L, Xu Z, Dryer SE (1998) Arachidonic acid-sensitive A-currents and multiple Kv4 transcripts are expressed in chick ciliary ganglion neurons. Brain Res 789:162–166.

Duerson K, White RE, Jiang F, Schonbrunn A, Armstrong DL (1996) Somatostatin stimulates BK_{Ca} channels in rat pituitary tumor cells through lipoxygenase metabolites of arachidonic acid. Neuropharmacology 35:949–961.

Hoffman DA, Johnston D (1998) Downregulation of transient K^+ channels in dendrites of hippocampal CA1 pyramidal neurons by activation of PKA and PKC. J Neurosci 18:3521–3528.

Hoffman DA, Johnston D (1999) Neuromodulation of dendritic action potentials. J Neurophysiol 81:408–411.

Hoffman DA, Magee JC, Colbert CM, Johnston D (1997) K^+ channel regulation of signal propagation in dendrites of hippocampal pyramidal neurons. Nature 387:869–875.

Horimoto N, Nabekura J, Ogawa T (1997) Arachidonic acid activation of potassium channels in rat visual cortex neurons. Neuroscience 77:661–671.

Jaffe DB, Johnston D, Lasser-Ross N, Lisman JE, Miyakawa H, Ross WN (1992) The spread of Na^+ spikes determines the pattern of dendritic Ca^{2+} entry into hippocampal neurons. Nature 357:244–246.

Keros S, McBain CJ (1997) Arachidonic acid inhibits transient potassium currents and broadens action potentials during electrographic seizures in hippocampal pyramidal and inhibitory interneurons. J Neurosci 17:3476–3487.

Keyser DO, Alger BE (1990) Arachidonic acid modulates hippocampal calcium current via protein kinase C and oxygen radicals. Neuron 5:545–553.

Kim D, Clapham DE (1989) Potassium channels in cardiac cells activated by arachidonic acid and phospholipids. Science 244:1174–1176.

Magee JC, Johnston D (1997) A synaptically controlled, associative signal for hebbian plasticity in hippocampal neurons. Science 275:209–213.

Magee J, Hoffman D, Colbert C, Johnston D (1998) Electrical and calcium signaling in dendrites of hippocampal pyramidal neurons. Annu Rev Physiol 60:327–346.

Maletic-Savatic M, Lenn NJ, Trimmer JS (1995) Differential spatiotemporal expression of K^+ channel polypeptides in rat hippocampal neurons developing *in situ* and *in vitro*. J Neurosci 15:3840–3851.

Markram H, Lübke J, Frotscher M, Sakmann B (1997) Regulation of synaptic efficacy by coincidence of postsynaptic APs and EPSPs. Science 275:213–215.

McGahon B, Lynch MA (1996) The synergism between metabotropic glutamate receptor activation and arachidonic acid on glutamate release is occluded by induction of long-term potentiation in the dentate gyrus. Neuroscience 72:847–855.

McGahon B, Clements MP, Lynch MA (1997) The ability of aged rats to sustain long-term potentiation is restored when the age-related decrease in membrane arachidonic acid concentration is reversed. Neuroscience 81:9–16.

Meves H (1994) Modulation of ion channels by arachidonic acid. Prog Neurobiol 43:175–186.

Miller B, Sarantis M, Traynelis SF, Attwell D (1992) Potentiation of NMDA receptor currents by arachidonic acid. Nature 355:722–725.

Ordway RW, Walsh, Jr. JV, Singer JJ (1989) Arachidonic acid and other fatty acids directly activate potassium channels in smooth muscle cells. Science 244:1176–1179.

Schweitzer P, Madamba S, Siggins GR (1990) Arachidonic acid metabolites as mediators of somatostatin-induced increase of neuronal M-current. Nature 346:464–467.

Serôdio P, Miera EV-SD, Rudy B (1996) Cloning of a novel component of A-type K^+ channels operating a subthreshold potentials with unique expression in heart and brain. J Neurophysiol 75:2174–2179.

Sheng M, Tsaur M-L, Jan YN, Jan LY (1992) Subcellular segregation of two A-type K^+ channel proteins in rat central neurons. Neuron 9:271–284.

Spruston N, Schiller Y, Stuart G, Sakmann B (1995) Activity-dependent action potential invasion and calcium influx into hippocampal CA1 dendrites. Science 268:297–300.

Stuart GJ, Sakmann B (1994) Active propagation of somatic action potentials into neocortical pyramidal cell dendrites. Nature 367:69–72.

Stuart GJ, Dodt HU, Sakmann B (1993) Patch-clamp recordings from the soma and dendrites of neurones in brain slices using infrared video microscopy. Pflügers Arch 423:511–518.

Stuart G, Spruston N, Sakmann B, Häusser M (1997) Action potential initiation and backpropagation in neurons of the mammalian CNS. Trends Neurosci 20:125–131.

Svoboda K, Denk W, Kleinfeld D, Tank DW (1997) In vivo dendritic calcium dynamics in neocortical pyramidal neurons. Nature 385:161–165.

Tsubokawa H, Ross WN (1996) IPSPs modulate spike backpropagation and associated $[Ca^{2+}]_i$ changes in the dendrites of hippocampal CA1 pyramidal neurons. J Neurophysiol 76:2896–2906.

Tsubokawa H, Ross WN (1997) Muscarinic modulation of spike backpropagation in the apical dendrites of hippocampal CA1 pyramidal neurons. J Neurosci 17:5782–5791.

Turner RW, Meyers DER, Richardson TL, Barker JL (1991) The site for initiation of action potential discharge over the somatodendritic axis of rat hippocampal CA1 pyramidal neurons. J Neurosci 11:2270–2280.

Villarroel A, Schwarz TL (1996) Inhibition of the Kv4 (Shal) family of transient K^+ currents by arachidonic acid. J Neurosci 16:1016–1025.